

An introduction to real-time renormalization group

Herbert Schoeller^{1,2}

¹ Forschungszentrum Karlsruhe, Institut für Nanotechnologie, 76021 Karlsruhe, Germany

² Institut für Theoretische Festkörperphysik, Universität Karlsruhe, 76128 Karlsruhe, Germany

1 Introduction

This article presents a tutorial introduction to a recently developed real-time renormalization group method [1]. It describes nonequilibrium properties of discrete quantum systems coupled linearly to an environment. We illustrate the technique by a simple and exactly solvable model: A quantum dot consisting of a single non-degenerate level coupled to two reservoirs. The article is intended for advanced students. Besides elementary quantum mechanics and statistical mechanics, it requires knowledge of second quantization and Wick's theorem. The latter topics can be learned easily from standard textbooks, see e.g. Ref. [2].

Renormalization group (RG) methods are standard tools to describe various aspects of condensed matter problems beyond perturbation theory [3]. Many impurity problems have been treated by numerical RG with excellent results both for thermodynamic quantities and spectral densities [4,5]. These RG techniques, however, cannot describe nonequilibrium properties like the nonlinear conductance, the nonequilibrium stationary state, or the full time development of an initially out-of-equilibrium state. To address these aspects we present here a perturbative RG method, formulated for strongly correlated quantum systems with a finite number of states coupled linearly to external heat or particle reservoirs. Examples are: spin boson models, molecules interacting with electrodynamic fields, generalized Anderson-impurity models, quantum dot devices, magnetic nanoparticles interacting with phonons, etc.. Fundamentally new, we generate non-Hamiltonian dynamics during RG, which captures the physics of finite life times and dissipation. Furthermore, no initial or final cutoff in energy or time space is needed, i.e., large and small energy scales are accounted for correctly like in flow-equation methods [6]. Although correlation functions can also be studied, physical quantities like spin and charge susceptibilities or the current can be calculated directly without the need of nonequilibrium Green's functions.

The purpose of our RG technique is to describe quantum fluctuations which are induced by strong coupling between a small quantum system and an environment. There are several recent experiments which show the importance of quantum fluctuations in metallic single-electron transistors [7] and semiconductor quantum dots [8] (see [9] for an overview over theoretical papers). Due to the renormalization of resistance and local energy excitations, anomalous line

shapes of the conductance have been observed, which can not be explained by golden-rule theories. For applications of the real-time RG to these cases we refer to Rfs. [1,10].

Here we want to illustrate the method by an exactly solvable model, namely a quantum dot with one non-degenerate state with energy ϵ coupled to two reservoirs ($r = L, R$). The Hamiltonian $H = H_R + H_0 + H_T$ consists of three parts, corresponding to the reservoirs, the dot, and tunneling

$$H_R = \sum_r H_r = \sum_{kr} \epsilon_{kr} a_{kr}^\dagger a_{kr} , \quad (1)$$

$$H_0 = \epsilon c^\dagger c , \quad (2)$$

$$H_T = \sum_{kr} \left\{ T_r a_{kr}^\dagger c + T_r^* c^\dagger a_{kr} \right\} . \quad (3)$$

Nonequilibrium is taken into account by describing the electrons in the reservoirs by Fermi distribution functions with different electrochemical potentials μ_r . Tunneling is switched on suddenly at the initial time t_0 , i.e. initially the density matrix $\rho(t_0) = \rho_0$ decouples into an equilibrium part for each reservoir, $\rho_r = Z_r^{-1} e^{-\beta(H_r - \mu_r N_r)}$, and an arbitrary initial distribution $p(t_0) = p_0$ for the dot

$$\rho_0 = p_0 \rho_{res} = p_0 \rho_L \rho_{res} . \quad (4)$$

The aim is to calculate the time evolution of the reduced density matrix of the dot, $p(t) = Tr_{res} \rho(t)$, and the tunneling current $\langle I_r \rangle(t)$ flowing from reservoir r to the dot. The tunneling current operator is given by ¹

$$I_r = -e \dot{N}_r = ie \sum_k \left\{ T_r a_{kr}^\dagger c - T_r^* c^\dagger a_{kr} \right\} . \quad (5)$$

The solution of the above quadratic Hamiltonian is trivial since all degrees of freedom can easily be integrated out. Doing this by using Wick's theorem for all field operators within the Keldysh formalism, one can easily solve the full nonequilibrium problem [11]. However, except for having solved a special and almost trivial problem, we would not have gained anything for solving more general problems of dissipative quantum mechanics. Usually, the local system can not be integrated out due to interaction terms or spin degrees of freedom. Therefore, we try to proceed differently. We will only integrate out the reservoirs and keep the dot degrees of freedom explicitly. This is always possible for an effectively noninteracting bath. As a result, we get an effective theory in terms of the local degrees of freedom, expressed by a formally exact kinetic equation for the reduced density matrix of the dot. For the special Hamiltonian (1)-(3), we solve this equation exactly. Furthermore, we will also develop a renormalization group method to solve the kinetic equation. We show that the RG equations describe the same exact solution. The important point is that both steps, i.e. (a) setting up the kinetic equation, and (b) setting up the RG equations, are

¹ Throughout this work we set $\hbar = k_B = 1$ and use $e < 0$

not specific to the above Hamiltonian but can be applied to any discrete quantum system coupled linearly to an environment. The only difference is that, for most problems, the resulting RG equations have to be solved numerically. In conclusion, the above Hamiltonian serves as a test example to illustrate the RG technique and to demonstrate that it is well-defined and useful.

2 Diagrammatic language

2.1 Diagrams on the Keldysh contour

We start by introducing some convenient notations. The index $\mu = \eta r$ labels the possible tunneling processes between reservoirs and dot. $\eta = \pm$ indicates tunneling in/out, and $r = L, R$ specifies the reservoir. We define the following reservoir and dot operators

$$j_{-r} = \sum_k T_r a_{kr}^\dagger, \quad j_{+r} = \sum_k T_r^* a_{kr}, \quad (6)$$

$$g_{-r} = c, \quad g_{+r} = c^\dagger. \quad (7)$$

We denote the two possible states of the dot by $s = 0, 1$ with energies $E_0 = 0$ and $E_1 = \epsilon$. The Hamiltonian (1)-(3) becomes

$$H_R = \sum_r \epsilon_{kr} a_{kr}^\dagger a_{kr}, \quad (8)$$

$$H_0 = \sum_s E_s |s\rangle \langle s|, \quad (9)$$

$$H_T = \sum_\mu : g_\mu j_\mu := \sum_r \{g_{+r} j_{+r} + j_{-r} g_{-r}\}, \quad (10)$$

where the symbol $: \dots :$ denotes normal ordering of Fermi field operators but without sign change when two operators are interchanged. The current operator (5) for the left reservoir is given by

$$I_L = \sum_\mu : i_\mu j_\mu :, \quad i_\mu = -ie\eta g_\mu \delta_{rL}, \quad (\mu = \eta r), \quad (11)$$

and a corresponding equation for I_R .

The time evolution of an arbitrary observable a follows from the von Neumann equation

$$\langle a \rangle(t) = Tr a \rho(t) = Tr a e^{-iH(t-t_0)} \rho_0 e^{iH(t-t_0)} \quad (12)$$

$$= Tr e^{iH(t-t_0)} a e^{-iH(t-t_0)} \rho_0, \quad (13)$$

where, in the last step, we have used cyclic invariance under the trace. To get a matrix element of the reduced density matrix of the dot, $p(t)_{ss'} = \langle a \rangle(t)$, we need $a = |s'\rangle \langle s|$. For the current, we take $a = I_L = \sum_\mu : i_\mu j_\mu :$.

To integrate out the reservoirs, we expand the propagators in tunneling and apply Wick's theorem to the reservoir degrees of freedom. We introduce the interaction picture

$$b(t) = e^{i(H_R+H_0)(t-t_0)} b e^{-i(H_R+H_0)(t-t_0)} , \quad (14)$$

and obtain

$$e^{iH(t-t_0)} a e^{-iH(t-t_0)} = \tilde{T} e^{i \int_{t_0}^t dt' H_T(t')} a(t) T e^{-i \int_{t_0}^t dt' H_T(t')} , \quad (15)$$

where T and \tilde{T} denote the time-ordering and anti-time-ordering operators, respectively. Inserting (15) in (13) and expanding in H_T gives a series of terms which we visualize diagrammatically, see Fig. 1. The upper (lower) line corresponds to the forward (backward) propagator. The diagram shown corresponds to the following expression

$$i^2 (-i)^2 \text{Tr} H_T(t_3) H_T(t_2) a(t) H_T(t_1) H_T(t_4) \rho_0 . \quad (16)$$

We see that the operators are ordered along a closed time path (Keldysh contour), as shown in Fig. 1.

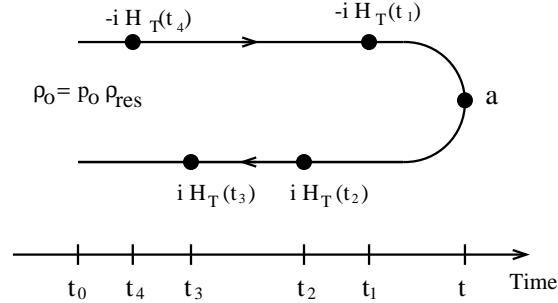


Fig. 1. Diagram corresponding to Eq. (16).

The next step is to insert $H_T = \sum_{\mu} : g_{\mu} j_{\mu} :$ for the tunneling Hamiltonian and $\rho_0 = \rho_0 \rho_{res}$ for the initial density matrix. We use the short-hand notation $g_i = g_{\mu_i}(t_i)$ and $j_i = j_{\mu_i}(t_i)$, and decompose each diagram into a dot and reservoir part. If $a = |s' \rangle \langle s|$ is a dot operator, we get from (16)

$$i^2 (-i)^2 \sum_{\mu_1 \mu_2 \mu_3 \mu_4} \{ \text{Tr}_0 g_3 g_2 a(t) g_1 g_4 \rho_0 \} \{ \text{Tr}_{res} j_3 j_2 j_1 j_4 \rho_{res} \} , \quad (17)$$

whereas, if $a = I_L = \sum_{\mu} : i_{\mu} j_{\mu} :$ is the current operator, we get

$$i^2 (-i)^2 \sum_{\mu \mu_1 \mu_2 \mu_3 \mu_4} \{ \text{Tr}_0 g_3 g_2 i_{\mu}(t) g_1 g_4 \rho_0 \} \{ \text{Tr}_{res} j_3 j_2 j_{\mu}(t) j_1 j_4 \rho_{res} \} . \quad (18)$$

Here, Tr_0 (Tr_{res}) denotes the trace over the dot (reservoir) degrees of freedom. The reader can convince himself very easily that this factorization does not imply any additional minus signs from commutation of Fermi operators. The reason is the quadratic form of the tunneling Hamiltonian.

The trace over the reservoirs can be calculated easily by using Wick's theorem [2]. As a result, we can decompose any average over products of reservoir field operators into a sum over products of pair contractions. Denoting by $\langle \dots \rangle$ the average over the reservoirs, we get for the reservoir part of (17)

$$\begin{aligned} \langle j_3 j_2 j_1 j_4 \rangle &= \overbrace{j_3 j_2 j_1 j_4} + \overbrace{j_3 j_2 j_1 j_4} + \overbrace{j_3 j_2 j_1 j_4} \\ &= \langle j_3 j_2 \rangle \langle j_1 j_4 \rangle - \langle j_3 j_1 \rangle \langle j_2 j_4 \rangle + \langle j_3 j_4 \rangle \langle j_2 j_1 \rangle . \end{aligned} \quad (19)$$

Each pair contraction corresponds to an equilibrium average over two reservoir field operators. If two contractions intersect proper minus signs have to be taken into account due to Fermi statistics. A pair contraction $\langle j_\mu(t) j_{\mu'}(t') \rangle$ depends on the relative time $t - t'$ and is only non-zero for $\mu' = \bar{\mu}$, with $\bar{\mu} = -\eta r$ (if $\mu = \eta r$). We define

$$\gamma_\mu(t) = \langle j_{\bar{\mu}}(t) j_\mu \rangle , \quad (20)$$

and get, by using the definition (6)

$$\begin{aligned} \gamma_\mu(t) &= \sum_k |T_r|^2 \begin{cases} \langle a_{kr}^\dagger(t) a_{kr} \rangle & \text{for } \eta = + \\ \langle a_{kr}(t) a_{kr}^\dagger \rangle & \text{for } \eta = - \end{cases} \\ &= \frac{1}{2\pi} \int dE \Gamma_r(E) e^{i\eta E t} f^\eta(E - \mu_r) \end{aligned} \quad (21)$$

$$\cong \frac{\Gamma_r}{2\pi} \int dE e^{\eta(E - \mu_r)/D} e^{i\eta E t} f_r^\eta(E) . \quad (22)$$

Here we have defined

$$\Gamma_r \cong \Gamma_r(E) = 2\pi \sum_k |T_r|^2 \delta(E - \epsilon_{kr}) = 2\pi |T_r|^2 N_r(E) , \quad (23)$$

with $N_r(E)$ being the density of states of reservoir r . We define $f^+ = f$, $f^- = 1 - f$, and $f_r^\eta(E) = f^\eta(E - \mu_r)$, with $f(E) = 1/(\exp(\beta E) + 1)$ being the Fermi function, and $\beta = 1/T$ the inverse temperature. We take the density of states $N_r(E)$ independent of energy and regularize the integral (21) by introducing an exponential convergence factor $e^{\eta(E - \mu_r)/D}$. Here, D corresponds to a high energy cutoff. In the end, we will send $D \rightarrow \infty$. Performing the integral (22) gives

$$\gamma_\mu(t) = \frac{-i\Gamma_r e^{i\eta\mu_r t}}{2\beta \sinh[\pi(t - i/D)/\beta]} . \quad (24)$$

Furthermore, we define

$$\gamma_r^\eta(t) = \gamma_\mu(\eta t) , \quad (25)$$

and note the important property

$$\lim_{D \rightarrow \infty} \{ \gamma_r^+(t) + \gamma_r^-(t) \} = \Gamma_r \delta(t) , \quad (26)$$

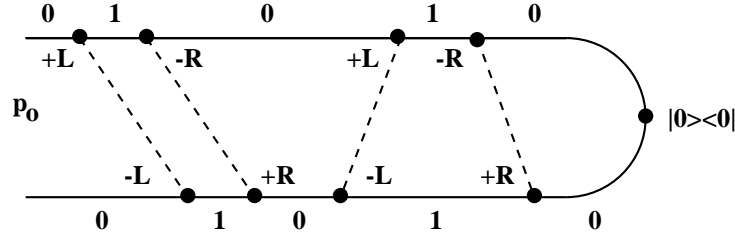


Fig. 2. Diagram after the application of Wick's theorem. On the propagators the states $s = 0, 1$ of the dot are shown. At the vertices we have indicated the index $\mu = \eta r$.

which follows directly from (22).

We indicate the pair contractions diagrammatically by connecting the corresponding vertices by a dashed line, see Fig. 2. The remaining part for the dot degrees of freedom still remains, see Eq. (17). We calculate this part by inserting intermediate states of the dot between the operators. These states are indicated in Fig. 2 between the tunneling vertices. The reservoirs are already integrated out, so the tunneling vertices correspond to the dot operators g_{μ_i} (with an additional factor $\mp i$ for a vertex on the upper (lower) propagator). Between the tunneling vertices we have the free time evolution of the dot, i.e. for a propagation of state s from t_2 to t_1 , we get an exponential factor $e^{-iE_s(t_1-t_2)}$.

Our diagrammatic language provides an effective description in terms of the dot degrees of freedom. The presence of the reservoirs is reflected by the retarded coupling of the tunneling vertices by the free Green's function of the reservoirs. In particular, this means that the forward and backward propagator are no longer independent but are coupled by reservoir lines. We will see in section 3.1 that this leads to rates in a kinetic equation for $p(t)$.

2.2 Superoperator notation

In this section we will replace the double-propagator diagrams on the Keldysh contour by a convenient matrix notation. This provides a very compact and analytic way to express diagrams by formulas.

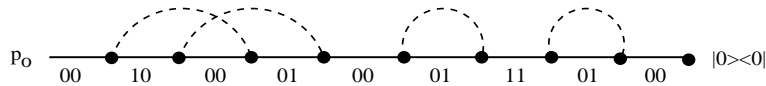


Fig. 3. Diagram in the double-state representation. It results from Fig. 2 by taking the upper and lower line together to one single line.

Instead of considering two propagators and specifying the dot states on each propagator separately, we can formally take both propagators together to one line and specify the state on this new propagator by a double dot state (s, s') , see Fig. 3. Here, the first (second) state corresponds to the state on the upper (lower) propagator. By this trick we have lost the information whether a tunneling

vertex lies on the upper or lower propagator. To recover this we add to the index μ of the tunneling vertex operator an additional index $p = \pm$, which indicates whether g_μ acts on the upper (lower) propagator. The new vertex is denoted by G_μ^p with matrix elements

$$(G_\mu^+)_{s_1 s'_1, s_2 s'_2} = -i(g_\mu)_{s_1 s_2} \delta_{s'_1 s'_2} \quad (27)$$

$$(G_\mu^-)_{s_1 s'_1, s_2 s'_2} = i\delta_{s_1 s_2} (g_\mu)_{s'_2 s'_1} . \quad (28)$$

We have included the factors $\mp i$ for a vertex on the upper (lower) propagator into the definition of G_μ^p . The free time evolution between the vertices is given by a factor $e^{-i(E_s - E_{s'})(t_1 - t_2)}$, where (s, s') indicates the double state on the line. This can be written in operator form as $(e^{-iL_0(t_1 - t_2)})_{ss', ss'}$, with

$$(L_0)_{s_1 s'_1, s_2 s'_2} = \delta_{s_1 s_2} \delta_{s'_1 s'_2} (E_{s_1} - E_{s'_1}) . \quad (29)$$

Finally, a contraction connecting a vertex $G_{\mu'}^{p'}$ at time t' with a vertex G_μ^p at time $t > t'$, is denoted by $\gamma_{\mu\mu'}^{pp'}(t - t')$. Using the definition (20) and the fact that operators on the lower propagator act always later than those on the upper propagator, we obtain

$$\gamma_{\mu\mu'}^{pp'}(t) = \delta_{\bar{\mu}, \mu'} \begin{cases} \langle j_\mu(t) j_{\bar{\mu}} \rangle = \gamma_{\bar{\mu}}(t) & \text{for } p' = + \\ \langle j_{\bar{\mu}} j_\mu(t) \rangle = \gamma_\mu(-t) & \text{for } p' = - \end{cases} \quad (30)$$

$$= \delta_{\bar{\mu}, \mu'} \frac{-i\Gamma_r e^{-i\eta\mu_r t}}{2\beta \sinh[\pi(p't - i/D)/\beta]} , \quad (31)$$

where we used the result (24) in the second step.

The double-state matrices L_0 and G_μ^p are called superoperators in the sense that they act on single-state matrices, i.e. on ordinary operators. If b is an ordinary operator, we can define L_0 and G_μ^p by

$$L_0 b = [H_0, b] \quad , \quad G_\mu^+ b = -i g_\mu b \quad , \quad G_\mu^- b = i b g_\mu . \quad (32)$$

Within the superoperator notation and using $a = |s'\rangle\langle s|$, an arbitrary diagram for $p_{ss'}(t)$ can be written as

$$p_{ss'}(t) \rightarrow \left\{ e^{-iL_0(t-t_0)} \overbrace{G_1 G_2 \dots G_n} p_0 \right\}_{ss'} . \quad (33)$$

The time dependence of $G_i = G_{\mu_i}^{p_i}(t_i)$ is defined by

$$G_\mu^p(t) = e^{iL_0(t-t_0)} G_\mu^p e^{-iL_0(t-t_0)} . \quad (34)$$

All operators $G_1 \dots G_n$ are coupled in all possible ways by reservoir pair contractions, as indicated in (33). Implicitly we assume summation over $\mu_1 \dots \mu_n$

and $p_1 \dots p_n$, together with the integration over the time variables $t_1 \dots t_n$ with $t > t_1 > t_2 > \dots > t_n > t_0$.

If $a = I_L = \sum_{\mu} : i_{\mu} \dot{j}_{\mu} :$ corresponds to the current operator, we get

$$\langle : i_{\mu} \dot{j}_{\mu} : \rangle(t) \rightarrow Tr_0 i_{\mu} \left\{ e^{-iL_0(t-t_0)} \overbrace{G_1 G_2 \dots G_n} \right\} p_0 . \quad (35)$$

In comparism to (33), we need an additional pair contraction to the current vertex. In order to treat the boundary vertex i_{μ} as well within the superoperator notation, we define a superoperator I_{μ}^p by

$$I_{\mu}^+ b = i_{\mu} b / 2 \quad , \quad I_{\mu}^- b = b i_{\mu} / 2 , \quad (36)$$

with matrix elements

$$(I_{\mu}^+)_{s_1 s'_1, s_2 s'_2} = \frac{1}{2} (i_{\mu})_{s_1 s_2} \delta_{s'_1 s'_2} \quad , \quad (I_{\mu}^-)_{s_1 s'_1, s_2 s'_2} = \frac{1}{2} \delta_{s_1 s_2} (i_{\mu})_{s'_2 s'_1} . \quad (37)$$

Using cyclic invariance under the trace, we get for (35)

$$\langle : i_{\mu} \dot{j}_{\mu} : \rangle(t) \rightarrow Tr_0 I_t \overbrace{G_1 G_2 \dots G_n} p_0 , \quad (38)$$

where $I_t = I_{\mu}^p(t)$, and the interaction picture is defined by

$$I_{\mu}^p(t) = I_{\mu}^p e^{-iL_0(t-t_0)} . \quad (39)$$

Eqs. (33) and (38) are the central result of this section. They relate the reduced density matrix of the dot and the average current to diagrammatic expressions in a very compact and analytic way. It turns out that the usage of superoperators simplifies the notation considerably. We will see in sections 3 and 4 that the derivation of kinetic equations and renormalization group equations is very transparent in this language. However, one should always keep in mind that the usage of superoperators is only a formal trick to find a convenient matrix notation. Therefore, we have set up the diagrammatic representation in terms of the Keldysh contour first, and then, in a second step, introduced the superoperators. Of course it is also possible to start directly with superoperators [1], which provides a more compact and shorter way to arrive at Eqs. (33) and (38). However, for pedagogical and physical reasons, we did not proceed in this way here. The diagrams on the Keldysh contour reveal better that there are different kinds of terms which have to be distinguished very carefully from a physical point of view. Reservoir lines connecting the upper and lower propagator correspond to rates, they change the state of the dot simultaneously on the upper *and* the lower propagator. This describes a transition from one diagonal matrix element of the reduced density matrix $p(t)$ to another one. Such processes can not be expressed on a Hamiltonian level and lead basically to the physics of dissipation. In contrast, reservoir contractions which connect vertices within the upper or lower propagator describe renormalization and broadening of levels.

3 Kinetic equation

3.1 General approach

In this section we will derive a self-consistent equation for the reduced density matrix $p(t)$ of the dot, together with an expression for the average current. To achieve this it is essential to distinguish in Eqs. (33) and (38) between connected and disconnected parts. From (33) we see that any diagram for $p(t)$ can be written in the form

$$e^{-iL_0(t-t_1)} (A_1 G \dots GB_2)_{con} e^{-iL_0(t_2-t_3)} (A_3 G \dots GB_4)_{con} \dots \\ \dots e^{-iL_0(t_{2n-2}-t_{2n-1})} (A_{2n-1} G \dots GB_{2n})_{con} e^{-iL_0(t_{2n}-t_0)} p_0 . \quad (40)$$

Here, $(A_i G \dots GB_{i+1})_{con}$ denotes a sequence of vertices between t_{i+1} and t_i which are coupled by pair contractions in such a way that any vertical cut between t_{i+1} and t_i will cross some contraction. We define such a block as a connected part of a diagram. E.g. Fig. 3 shows a sequence of three connected blocks. The boundary vertices A and B are identical to G , i.e. $A_\mu^p = B_\mu^p = G_\mu^p$, but the interaction picture is defined differently

$$A_\mu^p(t) = A_\mu^p e^{-iL_0(t-t_0)} \quad , \quad B_\mu^p(t) = e^{iL_0(t-t_0)} B_\mu^p . \quad (41)$$

The reason is that we want the connected part $(A_i G \dots GB_{i+1})_{con}$ of a diagram to depend only on the relative time argument $t_i - t_{i+1}$. Furthermore, we distinguish the boundary vertices A_μ^p and B_μ^p from G_μ^p since, within the renormalization group procedure developed in section 4, the boundary vertices renormalize differently.

We define the sum over all connected diagrams between t' and t by the kernel $\Sigma(t - t')$

$$\Sigma(t - t') \quad \rightarrow \quad (A_t G_1 G_2 \dots G_{2n} B_{t'})_{con} . \quad (42)$$

We note the important property that the kernel $\Sigma(t - t')$ is independent of the initial time t_0 since all exponential factors $e^{\pm iL_0 t_0}$ arising from the interaction picture cancel within Σ . Thus, in order to calculate Σ , we can set $t_0 = 0$ in the definition of the interaction picture of A , B , and G , see Eqs. (34) and (41).

Using the definition (42) for Σ in (40), we obtain

$$p(t) = e^{-iL_0(t-t_0)} p_0 + \sum_{n=1}^{\infty} \int_{t_0}^t dt_1 \int_{t_0}^{t_1} dt_2 \dots \int_{t_0}^{t_{2n-1}} dt_{2n} \\ e^{-iL_0(t-t_1)} \Sigma(t_1 - t_2) e^{-iL_0(t_2-t_3)} \Sigma(t_3 - t_4) \dots \\ \dots e^{-iL_0(t_{2n-2}-t_{2n-1})} \Sigma(t_{2n-1} - t_{2n}) e^{-iL_0(t_{2n}-t_0)} p_0 . \quad (43)$$

Differentiating with respect to time gives the kinetic equation

$$\dot{p}(t) + iL_0 p(t) = \int_{t_0}^t dt' \Sigma(t - t') p(t') . \quad (44)$$

Since the r.h.s. of this equation is a convolution in time space, we can formally solve this equation in Laplace space. We define the Laplace transform by

$$\tilde{p}(z) = \int_{t_0}^{\infty} dt e^{izt} p(t) \quad , \quad \tilde{\Sigma}(z) = \int_0^{\infty} dt e^{izt} \Sigma(t) \quad , \quad (45)$$

and get from (44) the solution

$$\tilde{p}(z) = \frac{i}{z - L_0 - i\tilde{\Sigma}(z)} p_0 \quad . \quad (46)$$

The time dependence $p(t)$ follows by reversing the Laplace transform

$$p(t) = \lim_{\eta \rightarrow 0} \frac{1}{2\pi} \int_{-\infty+i\eta}^{\infty+i\eta} dz e^{-izt} \tilde{p}(z) = \lim_{\eta \rightarrow 0} \frac{1}{2\pi} \int_{-\infty}^{\infty} d\omega e^{-i\omega t} \tilde{p}(\omega + i\eta) \quad . \quad (47)$$

We remark that $\tilde{p}(z)$, defined by (45), is analytic in the upper half plane since $p(t)$ will approach a stationary value for $t \rightarrow \infty$. Thus, within the integration region of (47) the integrand is well-defined. We see that the integral kernel $\tilde{\Sigma}(z)$ is the central object which has to be calculated. The full time evolution of $p(t)$ out of an arbitrary nonequilibrium state can be obtained once $\tilde{\Sigma}(z)$ is known for all $z = \omega + i0^+$. The calculation of $\tilde{\Sigma}(z)$ will be the subject of the renormalization group approach described in section 4.

The stationary state is defined by

$$p_{st} = \lim_{t \rightarrow \infty} p(t) = -i \lim_{z \rightarrow i0^+} z \tilde{p}(z) \quad . \quad (48)$$

Multiplying (46) by $z[z - L_0 - i\tilde{\Sigma}(z)]$ and taking the limit $z \rightarrow i0^+$, we see that the stationary state is the eigenvector of $L_0 + i\tilde{\Sigma}(i0^+)$ with eigenvalue zero

$$[L_0 + \tilde{\Sigma}(i0^+)] p_{st} = 0 \quad . \quad (49)$$

The density matrix $p(t)$ is hermitian. In Laplace space this is equivalent to

$$\tilde{p}(z)_{s's'}^* = \tilde{p}(-z^*)_{s's} \quad . \quad (50)$$

This follows from the solution (46) by using the symmetry relations

$$(iL_0)_{s_1 s'_1, s_2 s'_2}^* = (iL_0)_{s'_1 s_1, s'_2 s_2} \quad , \quad (G_{\mu}^p)_{s_1 s'_1, s_2 s'_2}^* = (G_{\mu}^{\bar{p}})_{s'_1 s_1, s'_2 s_2} \quad , \quad (51)$$

where $\bar{p} = -p$. They follow directly from (27), (28), (29), and the hermiticity of the Hamiltonian. The consequence for the kernel (42) is

$$\Sigma(t)_{s_1 s'_1, s_2 s'_2}^* = \Sigma(t)_{s'_1 s_1, s'_2 s_2} \quad , \quad \tilde{\Sigma}(z)_{s_1 s'_1, s_2 s'_2}^* = \tilde{\Sigma}(-z^*)_{s'_1 s_1, s'_2 s_2} \quad . \quad (52)$$

Using these relations together with the hermiticity of the initial density matrix p_0 , we find directly (50) from (46).

To prove conservation of probability $Tr_0 p(t) = 1$, we first note that

$$\sum_s (L_0)_{ss,\dots} = \sum_{sp} (A_\mu^p)_{ss,\dots} = \sum_{sp} (B_\mu^p)_{ss,\dots} = \sum_{sp} (G_\mu^p)_{ss,\dots} = 0 . \quad (53)$$

Applying this to (42) together with the fact that the contraction connected to the boundary operator A_μ^p does not depend on p , we find the same property for the kernel

$$\sum_s \Sigma(t)_{ss,\dots} = \sum_s \tilde{\Sigma}(z)_{ss,\dots} = 0 . \quad (54)$$

Applying Tr_0 to the kinetic equation (44), and using the properties (53) and (54), we find $d/dt Tr_0 p(t) = 0$ which proves conservation of probability.

To calculate the current we proceed analogously. From (38) and (40) we see that any diagram for the average current can be written as

$$Tr_0 (I_t G \dots G B_{t'})_{con} p(t') . \quad (55)$$

The first connected block contains the current vertex. The sum over all connected diagrams containing the current vertex is denoted by $\Sigma_I(t - t')$

$$\Sigma_I(t - t') \rightarrow (I_t G_1 G_2 \dots G_{2n} B_{t'})_{con} . \quad (56)$$

The only difference to (42) is that the boundary vertex A_μ^p has been replaced by the current vertex I_μ^p . From (55) and (56) we find

$$\langle I_L \rangle(t) = \sum_\mu \langle : i_\mu j_\mu : \rangle = \int_{t_0}^t dt' Tr_0 \Sigma_I(t - t') p(t') . \quad (57)$$

In Laplace space we get

$$\langle \tilde{I}_L \rangle(z) = Tr_0 \tilde{\Sigma}_I(z) \tilde{p}(z) , \quad (58)$$

and the stationary solution follows from

$$\langle I_L \rangle_{st} = Tr_0 \tilde{\Sigma}_I(i0^+) p_{st} . \quad (59)$$

The expectation value of the current is real, i.e. $\langle \tilde{I}_L \rangle(z)^* = \langle \tilde{I}_L \rangle(-z^*)$. This can be seen from the solution (58) by using the symmetry relations

$$(I_\mu^p)_{s_1 s'_1, s_2 s'_2}^* = (I_\mu^{\bar{p}})_{s'_1 s_1, s'_2 s_2} , \quad (60)$$

and

$$\Sigma_I(t)_{s_1 s'_1, s_2 s'_2}^* = \Sigma_I(t)_{s'_1 s_1, s'_2 s_2} \quad , \quad \tilde{\Sigma}_I(z)_{s_1 s'_1, s_2 s'_2}^* = \tilde{\Sigma}_I(-z^*)_{s'_1 s_1, s'_2 s_2} . \quad (61)$$

3.2 Exact solution

For the model of a single non-degenerate dot state, the kinetic equation and the current formula can be solved exactly. We derive this solution here and will check in section 5 that the renormalization group equations describe the same solution. If the reader is not interested in technical details, he can find the final results in Eqs. (65) and (74), and can proceed to the next section.

There are only two possible dot states $s = 0, 1$. We denote by \bar{s} the conjugate state, $\bar{s} = 1(0)$ if $s = 0(1)$. Furthermore we define $\bar{p} = -p$ and $\bar{\mu} = -\eta r$ if $\mu = \eta r$. The following three properties are needed for the following

$$\sum_{ps} (\overline{G_\mu^p})_{ss,\dots} = 0 \quad , \quad \sum_{ps} p (\overline{I_\mu^p})_{ss,\dots} = 0 \quad (62)$$

$$\sum_{pp'} (\overline{G_\mu^p G_{\mu'}^{p'}})_{s\bar{s},\dots} = 0 \quad (63)$$

$$\lim_{D \rightarrow \infty} \sum_{pp'} (\overline{G_\mu^p G_{\mu'}^{p'}})_{s\bar{s},\dots} = 0 \quad (64)$$

The time arguments of the interaction picture are not written explicitly. The proof can be found in the appendix.

For the reduced density matrix $p(t)$ and the current $\langle I_L \rangle(t)$, we need the kernels $\tilde{\Sigma}(z)$ and $\tilde{\Sigma}_I(z)$, see Eqs. (46) and (58). Due to particle number conservation of the total Hamiltonian, the reduced density matrix $p(t)$ stays diagonal if the initial density matrix p_0 is diagonal. We therefore need only the diagonal matrix elements $\tilde{\Sigma}(z)_{ss,s's'}$ and $\tilde{\Sigma}_I(z)_{ss,s's'}$ (the nondiagonal elements can also be calculated but do not contribute to the current due to Tr_0 in Eq. (58)).

The kernels are defined in (42) and (56). Using property (62) we find

$$\boxed{\begin{aligned} \tilde{\Sigma}(z)_{ss,ss} &= -\tilde{\Sigma}(z)_{\bar{s}\bar{s},ss} \quad , \\ \tilde{\Sigma}_I(z)_{ss,ss} &= \tilde{\Sigma}_I(z)_{\bar{s}\bar{s},ss} \quad . \end{aligned}} \quad (65)$$

As a consequence, we only have to calculate the matrix element (11, 00) of the kernels (the matrix element (00, 11) is analog and we quote the result at the end).

We call an intermediate double-propagator state ss "even", and a state $s\bar{s}$ "odd". The vertices G and I change the parity. We want the matrix element (11, 00), i.e. we start with an even state 11 from the left. Thus, the state after the first vertex of the kernels in Eqs. (42) and (56) is odd, and we can apply properties (63) and (64) for the pair of the second and third vertex. We see that the only possibility is that these two vertices are connected by a pair contraction. After these two vertices we are again in an odd state and can proceed in the same way. Finally we find that the only nonvanishing diagrams for $\tilde{\Sigma}(z)$ are

$$\overbrace{A \overline{GG} \overline{GG} \dots \overline{GG} B} \quad , \quad (66)$$

and analog for $\tilde{\Sigma}_I(z)$ by replacing $A \rightarrow I$.

We denote the sum over all sequences of \overline{GG} -blocks in (66) by $\Pi(t)$, where t is the time difference between the boundary vertices A and B . $\Pi(t)$ can be calculated analogously to section 3.1 where we resummed sequences of Σ -blocks with the result (46) for the reduced density matrix in Laplace space. Thus we obtain

$$\tilde{\Pi}(z) = \frac{i}{z - L_0 - i\tilde{\sigma}(z)}, \quad (67)$$

with

$$\sigma(t) = \overline{GG} = \gamma_{\mu\mu'}^{pp'}(t) G_\mu^p e^{-iL_0 t} G_{\mu'}^{p'}. \quad (68)$$

The kernels follow from

$$\Sigma(t) = \gamma_{\mu\mu'}^{pp'}(t) G_\mu^p \Pi(t) G_{\mu'}^{p'}, \quad (69)$$

$$\Sigma_I(t) = \gamma_{\mu\mu'}^{pp'}(t) I_\mu^p \Pi(t) G_{\mu'}^{p'}. \quad (70)$$

Using all definitions together with (26) and the fact that L_0 is a diagonal matrix, we find in the limit $D \rightarrow \infty$

$$\begin{aligned} \sigma(t)_{10,10} &= -\gamma^-(-t) - \gamma^+(-t) = -\Gamma \delta(t), \\ \tilde{\sigma}(z)_{10,10} &= -\Gamma/2, \\ \tilde{\Pi}(z)_{10,10} &= \frac{i}{z - (L_0)_{10,10} - i\tilde{\sigma}(z)_{10,10}} = \frac{i}{z - \epsilon + i\Gamma/2}, \\ \Pi(t)_{10,10} &= e^{-i\epsilon t} e^{-\Gamma t/2}, \end{aligned} \quad (71)$$

with $\gamma^\eta = \sum_r \gamma_r^\eta$ and $\Gamma = \sum_r \Gamma_r$. Furthermore, using the symmetry relations (51) we get $\Pi(t)_{01,01} = \Pi(t)_{10,10}^*$. Using these results together with $\gamma_r^\eta(t)^* = \gamma_r^\eta(-t)$, we can evaluate (69) and (70), and find

$$\Sigma(t)_{11,00} = \gamma^+(t) \Pi(t)_{10,10} + \text{h.c.} = \gamma^+(t) e^{-i\epsilon t} e^{-\Gamma t/2} + \text{h.c.} \quad (72)$$

$$\Sigma_I(t)_{11,00} = (e/2) \gamma_L^+(t) \Pi(t)_{10,10} + \text{h.c.} = (e/2) \gamma_L^+(t) e^{-i\epsilon t} e^{-\Gamma t/2} + \text{h.c.} \quad (73)$$

Using (22) and (25) we finally get in Laplace space

$$\boxed{\begin{aligned} \tilde{\Sigma}(z)_{11,00} &= \frac{i}{2\pi} \int dE \sum_r \Gamma_r f_r(E) \left\{ \frac{1}{E - \epsilon + z + i\Gamma/2} - \frac{1}{E - \epsilon - z - i\Gamma/2} \right\} \\ \tilde{\Sigma}_I(z)_{11,00} &= \frac{ie}{4\pi} \int dE \Gamma_L f_L(E) \left\{ \frac{1}{E - \epsilon + z + i\Gamma/2} - \frac{1}{E - \epsilon - z - i\Gamma/2} \right\} \end{aligned}} \quad (74)$$

By an analog calculation one obtains the matrix element (00, 11) by replacing $f_r \rightarrow 1 - f_r$ and changing the sign for the current kernel.

4 Renormalization group

In this section we will develop a renormalization group technique to calculate the kernels $\tilde{\Sigma}(z)$ and $\tilde{\Sigma}_I(z)$ in a systematic way beyond perturbation theory. The two kernels are defined in (42) and (56). Except for the first boundary vertex, they are formally the same. Therefore, w.l.o.g. we discuss in the following the kernel $\tilde{\Sigma}(z)$. Furthermore, as pointed out after Eq. (42), we can set $t_0 = 0$.

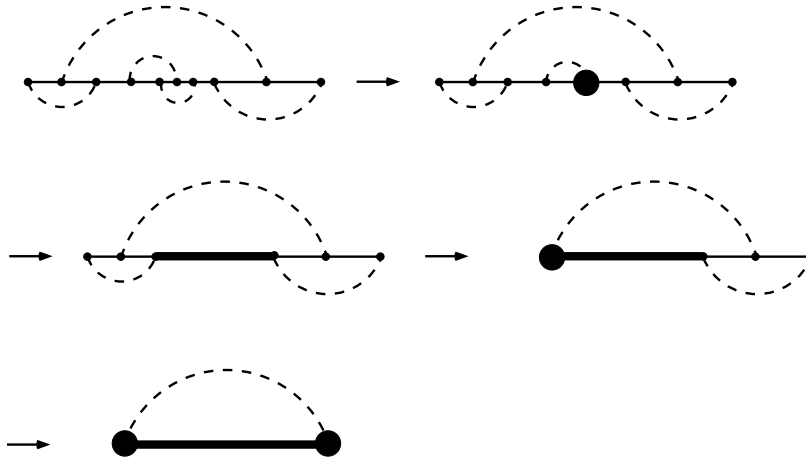


Fig. 4. Illustration of the RG-method. Successively, the shortest contraction line is integrated out. The thick lines and dots indicate renormalized propagators and vertices.

In section 2 we have found an effective theory in terms of the dot degrees of freedom. The reservoirs enter via pair contractions which couple the tunneling vertices. The aim is to integrate out all contractions in such a way that they can be interpreted as renormalization of L_0 , G , A and B . The procedure is shown schematically in Fig. 4. We start with the integration over the shortest contraction. This gives rise to a renormalization of G in Fig. 4. The integration over the next shortest contraction renormalizes the propagator $e^{-iL_0(t_1-t_2)}$ of the dot. Proceeding in the same way, we find a renormalization of A and B in the next two steps. Finally we are left with a diagram which we can calculate easily by perturbation theory but with renormalized quantities. It can also happen that two or more vertices fall into one contraction which is integrated out, see e.g. Fig. 5. In this case we generate double-, triple-, and higher order vertices. In a perturbative renormalization group treatment one cuts this infinite hierarchy at a certain level. Here, we only consider propagator and single-vertex renormalization.

As described, we first want to integrate over the short contraction lines, i.e. over short time scales of the function $\gamma_\mu(t)$. Short time scales correspond to large energy scales. This leads us to the usual way renormalization group is formulated. One introduces a cut-off function $F(E/D)$ in the integrand of (21), where D is a

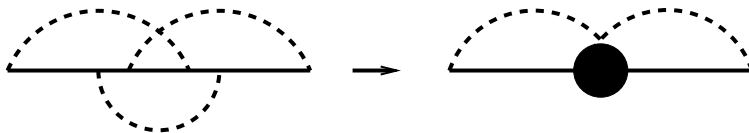


Fig. 5. Generation of a double-vertex.

high-energy cutoff, $F(0) = 1$ and $F(x)$ decays monotonically to zero sufficiently fast for $|x| \rightarrow \pm\infty$. As a consequence, the pair contraction $\gamma_{\mu,D}(t)$ depends on the cutoff D . In each renormalization group step one reduces the cutoff by an infinitesimal amount $D \rightarrow D - \delta D$, i.e. one tries to integrate out a small energy shell. The mathematical challenge is to interpret the result of this integration as a renormalization of system parameters, like L_0 , G , A and B .

We prefer to develop the renormalization group procedure in real-time space. This turns out to be easier and more systematic. We introduce a cut-off function $F(t/t_c)$ which cuts off small time scales, i.e. $F(x)$, with $x > 0$, is a monotonically increasing function with $F(0) = 0$ and $\lim_{x \rightarrow \infty} F(x) = 1$, see Fig. 6. t_c is a cutoff parameter for small time scales. We define a cutoff dependent reservoir contraction by

$$\gamma_{\mu,t_c}(t) = \gamma_{\mu}(t) F(t/t_c) . \quad (75)$$

If we choose a sharp cutoff function $F(x) = \Theta(x - 1)$, $\gamma_{\mu t_c}(t)$ includes only those time scales which are precisely larger than t_c . We note that the high-energy cutoff D introduced in Eq. (22) is independent of t_c and is not used as a renormalization group flow parameter. Within our real-time formulation, it corresponds to the physical band width of the reservoirs.

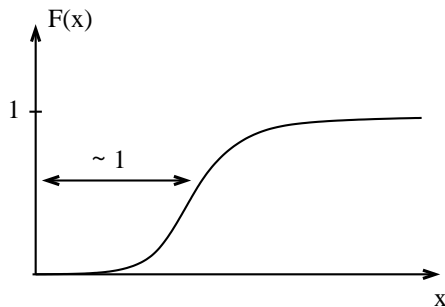


Fig. 6. The cutoff-function.

Motivated by the picture presented at the beginning of this section, we hope that all time scales being smaller than t_c , i.e. those being not present in $\gamma_{\mu t_c}(t)$ can be accounted for by renormalized quantities. To formulate this precisely let us write the kernel $\tilde{\Sigma}(z)$ as a functional of L_0 , G , A , B and γ

$$\tilde{\Sigma}(z) = \mathcal{F}(L_0, G_{\mu}^p, A_{\mu}^p, B_{\mu}^p, \gamma_{\mu}(t)) , \quad (76)$$

where $p, \mu,$ and t run over all possible values within the functional. After replacing γ_μ by the cutoff-dependent function $\gamma_{\mu t_c}$ inside this functional, we try to find a cutoff dependence of all other quantities in such a way that the kernel stays invariant with the *same* functional \mathcal{F}

$$\tilde{\Sigma}(z) = \tilde{\Sigma}_{t_c}(z) + \mathcal{F}(L_{0t_c}, G_{\mu t_c}^p, A_{\mu t_c}^p, B_{\mu t_c}^p, \gamma_{\mu t_c}(t)) . \quad (77)$$

This equation is only exact if we neglect higher order vertex corrections, as already pointed out above. Otherwise we have to include all higher-order vertex terms as arguments in the functional \mathcal{F} as well. Via $\gamma_{\mu t_c}$, the second term on the r.h.s includes only time scales which are larger than t_c . All other time scales are accounted for by the cutoff-dependence of $L_0, G, A,$ and B . The first term on the r.h.s contains the contributions where *all* time scales are smaller than t_c . This part is not included in the second term where at least one contraction line $\gamma_{\mu t_c}$ occurs. It is important to notice that $\tilde{\Sigma}_{t_c}(z)$ should not be viewed as being trivially defined by Eq. (77). If we choose a sharp cutoff function $F(x) = \Theta(x-1)$, $\tilde{\Sigma}_{t_c}(z)$ can be constructively defined as containing only those diagrams where *all* contraction lines have a length smaller than t_c . For $t_c \rightarrow \infty$ the second term on the r.h.s. of (77) vanishes, provided the function $\gamma_\mu(t)$ decays sufficiently fast for $t \rightarrow \infty$. Thus, we obtain the final solution from

$$\tilde{\Sigma}(z) = \lim_{t_c \rightarrow \infty} \tilde{\Sigma}_{t_c}(z) . \quad (78)$$

The aim is to find differential equations which describe the cutoff-dependence of $\tilde{\Sigma}_{t_c}(z), L_{0t_c}, G_{t_c}, A_{t_c}$ and B_{t_c} . This will be the subject of the rest of this section.

Let us increase the cutoff by an infinitesimal amount $t_c \rightarrow t_c + dt_c$. Due to the invariance, Eq. (77) should not change

$$0 = d\tilde{\Sigma}(z) + \mathcal{F}(L_0 + dL_0, G + dG, A + dA, B + dB, \gamma + d\gamma) , \quad (79)$$

where we have omitted the subindex t_c and the indices p and μ . The change of γ is known from the definition (75)

$$d\gamma_{\mu t_c}(t) = -\gamma_\mu(t) F'(t/t_c) t/t_c^2 dt_c , \quad (80)$$

or, for a sharp cutoff function $F(x) = \Theta(x-1)$

$$d\gamma_{\mu t_c}(t) = -\gamma_\mu(t_c) \delta(t-t_c) dt_c . \quad (81)$$

The increment $d\gamma$ in (79) leads to all diagrams where one contraction line is replaced by $d\gamma$. We indicate this by a cross and define

$$\overbrace{G_1 \dots G_2}^{\times} = - \left(\frac{d\gamma}{dt_c} \right)_{\mu\mu'}^{pp'}(t_1 - t_2) dt_c G_\mu^p(t_1) \dots G_{\mu'}^{p'}(t_2) , \quad (82)$$

We call this a "cross contraction". For a sharp cutoff function, we get

$$\overbrace{G_1 \dots G_2}^{\times} = \gamma_{\mu\mu'}^{pp'}(t_c) \delta(t_1 - t_2 - t_c) dt_c G_\mu^p(t_1) \dots G_{\mu'}^{p'}(t_2) . \quad (83)$$

Corresponding definitions hold for G replaced by A or B . By convention we have included a minus sign into the definition since $-d\gamma$ accounts for the time scales of the contraction between t_c and $t_c + dt_c$, compare Eq. (81). We have to identify all terms created by $d\gamma$ with a contribution arising either from $d\tilde{\Sigma}$, dL_0 , dG , dA or dB in Eq. (79) in order to fulfil invariance. Which one has to be taken depends on the number of vertices between G_1 and G_2 , and whether one or both of the vertices are boundary vertices.

Let us start with the simplest case of two successive vertices which are not at the boundary

$$G_1 \overleftrightarrow{G_2} G_3 G_4 . \quad (84)$$

Here, the two vertices G_1 and G_4 are contracted to any other vertices. Motivated by Fig. 4, it is tempting to take this diagram together with $G_1 G_4$ and interpret the cross contraction as a renormalization of L_0 in the following sense

$$\begin{aligned} G_1 G_4 &+ \int_{1>2>3>4} dt_2 dt_3 G_1 \overleftrightarrow{G_2} G_3 G_4 \\ &\stackrel{?}{=} e^{iL_0 t_1} G_{\mu_1}^{p_1} e^{-i(L_0 + dL_0)(t_1 - t_4)} G_{\mu_4}^{p_4} e^{-iL_0 t_4} . \end{aligned} \quad (85)$$

Expanding the exponential to linear order in dL_0 , we see that this requires the identity

$$\int_{1>2>3>4} dt_2 dt_3 G_1 \overleftrightarrow{G_2} G_3 G_4 \stackrel{?}{=} -i \int_{t_1 > t > t_4} dt G_1 (dL_0)(t) G_4 . \quad (86)$$

To obtain such a relation we see immediately a problem. The integrand of the l.h.s contains a two-time object $\overleftrightarrow{G_2} G_3$, whereas the integrand of the r.h.s contains the single-time object $(dL_0)(t)$. We have to decide to which time-variable we identify t . Let us make an arbitrary choice: $t \equiv t_3$. Then it is obvious to try the ansatz

$$-i (dL_0)(t_3) = \int_{2>3} dt_2 \overleftrightarrow{G_2} G_3 . \quad (87)$$

This is well-defined since it does not involve the time variables t_1 and t_4 . However, let us try to insert this ansatz into the r.h.s of (86). We get two terms

$$\begin{aligned} -i \int_{1>3>4} dt_3 G_1 (dL_0)(t_3) G_4 &= \int_{\substack{1>3>4 \\ 2>3}} dt_2 dt_3 G_1 \overleftrightarrow{G_2} G_3 G_4 \\ &= \int_{1>2>3>4} dt_2 dt_3 G_1 \overleftrightarrow{G_2} G_3 G_4 + \int_{2>1>3>4} dt_2 dt_3 G_1 \overleftrightarrow{G_2} G_3 G_4 \end{aligned} \quad (88)$$

The first term agrees with the l.h.s. of (86), whereas the second one is a correction term which has to be considered separately. Let us try to interpret it as a term

arising from dG . We define

$$(dG_{\mu_1}^{p_1})^{(1)}(t_1) = - \int_{2>1>3} dt_2 dt_3 G_1 \overleftrightarrow{G_2 G_3}, \quad (89)$$

where the subindex (1) indicates that this is the first contribution to dG (another one will follow below). Using this definition we finally get

$$\begin{aligned} \int_{1>2>3>4} dt_2 dt_3 G_1 \overleftrightarrow{G_2 G_3} G_4 &= -i \int_{1>3>4} dt_3 G_1 (dL_0)(t_3) G_4 + (dG_{\mu_1}^{p_1})^{(1)}(t_1) G_4 \\ &+ \int_{2>1>4>3} dt_2 dt_3 G_1 \overleftrightarrow{G_2 G_3} G_4. \end{aligned} \quad (90)$$

In the last term on the r.h.s. the two time-variables t_1 and t_4 are "clustered" together, they both have to lie within the time interval $[t_3, t_2]$. Therefore, we interpret this term as a double-vertex which we neglect. In conclusion, we have achieved our final goal: we have interpreted a term arising from $d\gamma$ by a renormalization of L_0 and G .

Let us try to understand what we have done so far and how to find a systematic procedure for obtaining the complete RG equations without going again into the details of the foregoing exercise. We have defined the renormalization of L_0 in (87), which is natural since this expression contains only operators of the dot. We write

$$-i(dL_0)(t_2) = \overleftrightarrow{G_1 G_2}, \quad (91)$$

where the arrow indicates the time variable which is not integrated out. It is *this* time variable which is used for the definition of the interaction picture of dL_0 and, most importantly, which is used for the definition of time-ordering, see the r.h.s of Eq. (86). The time-variable t_1 no longer appears explicitly because it is an internal integration variable within the definition of dL_0 . This has the consequence, that time variables of other vertices do not care about the value of t_1 regarding time ordering. E.g., if we multiply $(dL_0)(t_3)$ with a vertex G_2 from the left, time-ordering only requires $t_2 > t_3$ but the ordering of t_2 with respect to the internal integration variable t_1 is not prescribed. Thus, due to dL_0 , the following term will occur on the r.h.s. of (79)

$$\overleftrightarrow{G_2 G_1 G_3}, \quad (92)$$

where $t_1 > t_2 > t_3$. However, this term is not present in the original series because the ordering of operators does not agree with the ordering of time variables. Consequently, we have to subtract this term. This is the basic reason for the occurrence of the second term on the r.h.s. of (90).

We interpret minus the correction term (92) as renormalization of G . Again we have to specify the time variable for the interaction picture and for time-ordering. We choose t_2 in analogy to Eq. (89). Together with the "real" vertex

renormalization, arising from a free vertex inside a cross contraction, we get the complete renormalization of G

$$(dG_{\mu_2}^{p_2})(t_2) = \overbrace{G_1 G_2 G_3}^{\times} - G_2 \overbrace{G_1 G_3}^{\times} . \quad (93)$$

We can now proceed to look at other correction terms which can occur by multiplying (91) with two vertices from the left or (93) with one vertex from the left or right

$$\begin{array}{c} G_2 G_3 \overbrace{G_1 G_4}^{\times} + G_2 \overbrace{G_1 G_3 G_4}^{\times} - G_2 G_3 \overbrace{G_1 G_4}^{\times} + \overbrace{G_1 G_2 G_4 G_3}^{\times} - G_2 \overbrace{G_1 G_4 G_3}^{\times} , \end{array} \quad (94)$$

with $t_1 > t_2 > t_3 > t_4$. We have indicated the time-ordering variables of all sub-clusters which lead to these expressions. We see that the first and third term cancel each other. The other three correction terms have to be subtracted again. Minus the fifth term corresponds to the third term on the r.h.s. of Eq. (90). The second and fourth term are correction terms arising from the "real" vertex renormalization. However, all these correction terms correspond to double-vertices which we neglect consistently. Another double-vertex term arises from two free vertices within a cross contraction. Proceeding further in the same way, triple- and higher order vertex terms will occur which again are not considered here. We see that the procedure is very systematic and straightforward.

In the same way we can proceed for boundary vertices. Since we want to calculate the Laplace transform $\tilde{\Sigma}(z)$ of the kernel each diagram of the kernel (42) gets an additional factor e^{izt} . Consequently we define the interaction picture for the boundary vertices slightly different from (41). We simply include the factor from the Laplace transformation

$$A_{\mu}^p(t) = e^{izt} A_{\mu}^p e^{-iL_0 t} \quad , \quad B_{\mu}^p(t) = e^{iL_0 t} B_{\mu}^p e^{-izt} . \quad (95)$$

Analog to the above procedure we can write down immediately all terms with cross contractions containing boundary operators. They can be interpreted as renormalization of $\tilde{\Sigma}$, A and B

$$d\tilde{\Sigma}(z) = \overbrace{A_1 B_2}^{\times} |_{t_2=0} , \quad (96)$$

$$(dA_{\mu_2}^{p_2})(t_2) = \overbrace{A_1 G_2 G_3}^{\times} - A_2 \overbrace{G_1 G_3}^{\times} , \quad (97)$$

$$(dB_{\mu_2}^{p_2})(t_2) = \overbrace{G_1 G_2 B_3}^{\times} . \quad (98)$$

Again, we integrate implicitly over all time variables which are not indicated by an arrow, with $t_1 > t_2 > t_3$. Terms like $\overbrace{A_1 G_2}^{\times}$ or $\overbrace{G_1 B_2}^{\times}$ do not occur since they do not lead to connected diagrams. For this reason, there is also no correction term in the renormalization group equation for B .

Eqs. (91), (93), and (96)-(98) are the final RG-equations. They can be translated easily to get explicit expressions. In order to get the renormalization of the bare quantities we have to set $t_2 = 0$ in all equations. To account for possible

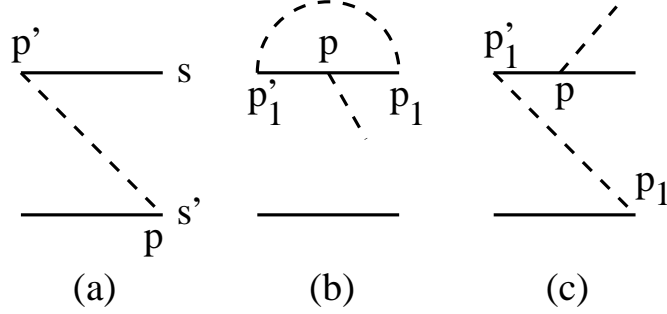


Fig. 7. Diagrams where additional minus occur if the ends of the indicated contraction are connected. In (a) a minus signs occurs if the particle number difference $N_s - N_{s'}$ is odd. In (b) and (c) a free vertex is crossed by connecting the end-points without crossing over p_0 .

minus signs arising from commutation of fermionic reservoir field operators, we have to include two auxiliary sign functions. They arise because we have to connect the two end points of the cross contraction. If the cross contraction couples the upper with the lower propagator, a minus sign occurs if the intermediate double-propagator state at the vertex with the larger time is odd (i.e. if the difference of the fermionic particle numbers on the upper and lower propagator is odd), see Fig. 7a. We account this by a sign operator $\hat{\sigma}_\mu^{pp'}$ multiplying each cross contraction from the left. The matrix elements of this operator are defined by

$$(\hat{\sigma}_\mu^{pp'})_{ss',ss'} = \begin{cases} pp' & \text{for } N_s - N_{s'} = \text{odd} \\ 1 & \text{for } N_s - N_{s'} = \text{even} \end{cases}, \quad (99)$$

where N_s is the fermionic particle number of state s and μ is a fermionic contraction (for bosonic contractions no additional sign has to be considered). The second sign function concerns the case when one free vertex occurs within a cross contraction. A minus sign occurs when the cross contraction crosses over the free vertex when we want to connect the two end points. Since $\hat{\sigma}$ is multiplied from the left by definition, we connect the vertices always in such a way that we do not cross over p_0 . We denote by p , p_1 , and p'_1 the indices of the free vertex, the vertex with the larger and the one with the smaller time variable of the cross contraction, respectively. If $p = p'_1$ we get an additional minus sign, see Fig. 7b and 7c. Therefore we multiply the "real" vertex correction by an additional sign function

$$\eta_{\mu\mu'_1}^{pp'_1} = \begin{cases} -pp'_1 & \text{for } \mu \text{ and } \mu' \text{ fermionic} \\ 1 & \text{otherwise} \end{cases}. \quad (100)$$

In summary we get the following RG equations

$$\begin{aligned}
 \frac{d}{dt_c} \tilde{\Sigma}(z) &= - \int_0^\infty dt \left(\frac{d\gamma}{dt_c} \right)_{\mu\mu'}^{pp'}(t) \hat{\sigma}_\mu^{pp'} A_\mu^p(t) B_{\mu'}^{p'} \\
 \frac{d}{dt_c} L_0 &= -i \int_0^\infty dt \left(\frac{d\gamma}{dt_c} \right)_{\mu\mu'}^{pp'}(t) \hat{\sigma}_\mu^{pp'} G_\mu^p(t) G_{\mu'}^{p'} \\
 \frac{d}{dt_c} G_\mu^p &= - \int_0^\infty dt \int_{-\infty}^0 dt' \left(\frac{d\gamma}{dt_c} \right)_{\mu_1\mu_1'}^{p_1p_1'}(t-t') \\
 &\quad \left[\eta_{\mu\mu_1}^{pp_1} \hat{\sigma}_{\mu_1}^{p_1p_1'} G_{\mu_1}^{p_1}(t) G_\mu^p - G_\mu^p \hat{\sigma}_{\mu_1}^{p_1p_1'} G_{\mu_1}^{p_1}(t) \right] G_{\mu_1'}^{p_1'}(t') \\
 \frac{d}{dt_c} A_\mu^p &= - \int_0^\infty dt \int_{-\infty}^0 dt' \left(\frac{d\gamma}{dt_c} \right)_{\mu_1\mu_1'}^{p_1p_1'}(t-t') \\
 &\quad \left[\eta_{\mu\mu_1}^{pp_1} \hat{\sigma}_{\mu_1}^{p_1p_1'} A_{\mu_1}^{p_1}(t) G_\mu^p - A_\mu^p \hat{\sigma}_{\mu_1}^{p_1p_1'} G_{\mu_1}^{p_1}(t) \right] G_{\mu_1'}^{p_1'}(t') \\
 \frac{d}{dt_c} B_\mu^p &= - \int_0^\infty dt \int_{-\infty}^0 dt' \left(\frac{d\gamma}{dt_c} \right)_{\mu_1\mu_1'}^{p_1p_1'}(t-t') \eta_{\mu\mu_1}^{pp_1} \hat{\sigma}_{\mu_1}^{p_1p_1'} G_{\mu_1}^{p_1}(t) G_\mu^p B_{\mu_1'}^{p_1'}(t')
 \end{aligned}
 \tag{101}$$

Implicitly we sum over all double indices on the r.h.s. of these equations which do not occur on the l.h.s.. We note that the overall sign on the r.h.s. differs from the one in [1] since we have included the factors $-i$ into the vertices. Furthermore, we have generalized the RG equations to an arbitrary cutoff-function $F(t/t_c)$. For a specific cutoff-function, e.g. $F(x) = \theta(x-1)$, and taking matrix elements of the RG-equations, all integrals in (101) can be calculated analytically. We are left with pure differential equations which can be solved numerically in a straightforward and very efficient way. Finally, the asymptotic value $\lim_{t_c \rightarrow \infty} \tilde{\Sigma}_{t_c}(z)$ gives the solution for the kernel, see Eq. (78). Using (46) and (47), we get the complete time-evolution of the reduced density matrix of the dot. The initial condition for the boundary operators at $t_c = 0$ is given by $A_\mu^p = B_\mu^p = G_\mu^p$. To get the current kernel $\tilde{\Sigma}_I(z)$, we take the same RG-equations with the initial conditions $A_\mu^p = I_\mu^p$ and $B_\mu^p = G_\mu^p$.

Numerically, one can not take the initial flow parameter $t_c^0 = 0$ and the final one $t_c^f \rightarrow \infty$. However, one can check that the final solution is stable for sufficiently small t_c^0 and large t_c^f . This means that $1/t_c^0$ and $1/t_c^f$ have to be much larger resp. smaller than all other energy scales

$$\frac{1}{t_c^f} \ll \Gamma_L, \Gamma_R, T, eV, |\epsilon| \ll D \ll \frac{1}{t_c^0}, \tag{102}$$

where $eV = \mu_L - \mu_R$ is the bias voltage, and Γ_L, Γ_R are defined in (23). In addition, we want to send the band-width cutoff $D \rightarrow \infty$. This means that we

have to check the stability of the solution for $t_c^0 \rightarrow 0$, $D \rightarrow \infty$, with $Dt_c^0 \rightarrow 0$. For the problem under consideration this is indeed possible.

There are three essential differences of our final RG equations to conventional poor man scaling and operator product expansion techniques [12,13]:

1. We have formulated the RG-equations within a real-time formalism on the Keldysh-contour.
2. We have not expanded the interaction picture of the vertex operators for small times, i.e. the renormalized propagation $\exp(\pm iL_0 t)$ is taken fully into account.
3. For $t_c > t_c^0$ we get $L_0 \neq [H_0, \cdot]$, i.e. we generate non-Hamiltonian dynamics during RG.

The first point is necessary for describing nonequilibrium phenomena. The second one is important for self-consistency reasons (L_0 in the exponent is a renormalized quantity) and for the stability of the solution for $t_c^f \rightarrow \infty$. Only if one expands the exponentials $\exp(\pm iL_0 t)$ in t , one has to stop the RG-flow when $|\lambda t_c| \sim 1$, where λ denotes any eigenvalue of L_0 . We do not need this expansion and, consequently, are able to integrate out all time scales. The third property is the most important one. It is essential for a nonequilibrium theory to describe the physics of dissipation. Thus, the renormalized superoperator L_0 should no longer be expressible by a commutator with a renormalized Hamiltonian H_0 , i.e. in matrix notation

$$(L_0)_{s_1 s_2, s'_1 s'_2} \neq (H_0)_{s_1 s_2} \delta_{s'_1 s'_2} - \delta_{s_1 s_2} (H_0)_{s'_2 s'_1} . \quad (103)$$

To show this let us first define the renormalized Hamiltonian in a natural way. It is obvious that contractions which connect the upper with the lower propagator of the Keldysh contour, do not lead to Hamiltonian dynamics. This was already explained at the end of section 2.2. Thus, in order to define the renormalized H_0 let us consider the same RG equations but allow only for contractions within the upper or lower propagator. Formally, this means $p = p'$ and $p_1 = p'_1$ in (101). Under these conditions we can write the solution as

$$(L_0)_{s_1 s_2, s'_1 s'_2} = (H_0)_{s_1 s_2} \delta_{s'_1 s'_2} - \delta_{s_1 s_2} (H_0^\dagger)_{s'_2 s'_1} . \quad (104)$$

To obtain this, we have used the symmetry relations (51) together with the property

$$\gamma_{\mu\mu'}^{pp'}(t)^* = \gamma_{\mu\mu'}^{pp'}(-t) = \gamma_{\bar{\mu}\bar{\mu}'}^{\bar{p}\bar{p}'}(t) . \quad (105)$$

The renormalized Hamiltonian H_0 is defined by considering only the upper propagator, i.e. setting $p = p' = p_1 = p'_1 = +$ and replacing $L_0 \rightarrow H_0$ and $G_\mu^+ \rightarrow -ig_\mu$

in the RG-equations. We note that H_0 is non-hermitian since we generate complex energies during RG. Physically this describes broadening of levels or finite life-times. From (104) we conclude that the backward propagator involves H_0^\dagger , i.e. the sign of energy-broadening is different for the forward and backward propagator. This means, that even if we disregard contractions connecting the upper with the lower propagator, we get $L_0 \neq [H_0, \cdot]$. However, this does not imply the physics of dissipation. It describes the physics of a finite broadening of the energy levels due to the coupling to the environment. This reflects the Heisenberg-uncertainty relationship.

In contrast, if we couple the forward and backward propagator by contractions, the matrix L_0 will completely change its form. It can neither be represented as (103) nor as (104). The coupling of the propagators gives rise to the generation of rates where the states on the upper and lower propagator are changed simultaneously. Rates describe the evolution of the system into a stationary state, i.e. we generate irreversibility or dissipation during RG.

The RG equations preserve conservation of probability and give real expectation values for hermitian observables. Once the symmetry relations and sum rules, stated in Eqs. (51)-(54) and (60)-(61), are fulfilled initially, they are not changed by the RG-flow. Thus, by applying the same proof as in section 3.1, we obtain a normalized probability distribution of the dot and a real expectation value for the current.

Under certain circumstances the RG equations can be simplified. This will be important for the exact solution presented in the next section. We decompose the pair contraction (20) trivially into two terms

$$\gamma_\mu(t) = \gamma_\mu^\delta(t) + \bar{\gamma}_\mu(t) , \quad (106)$$

with

$$\gamma_\mu^\delta = \frac{1}{2} \langle [j_{\bar{\mu}}(t), j_\mu]_{-\sigma} \rangle \quad , \quad \bar{\gamma}_\mu = \frac{1}{2} \langle [j_{\bar{\mu}}(t), j_\mu]_\sigma \rangle , \quad (107)$$

where $\sigma = \pm$ for $\mu =$ bosonic (fermionic), and $[\cdot, \cdot]_{-\sigma}$ denotes the (anti-)commutator for $\sigma = \pm$. This decomposition is useful since in many problems, the part $\gamma_\mu^\delta(t)$ turns out to be proportional to a delta function or derivatives of a delta function (at least for the band width cutoff $D \rightarrow \infty$). For our special model we get (compare (26))

$$\gamma_\mu^\delta(t) = \frac{\Gamma_r}{2} \delta(t) . \quad (108)$$

Such a contribution can be included into the initial conditions of the RG equations. First, we decompose $\gamma_{\mu\mu'}^{pp'}(t) = \gamma_{\mu\mu'}^{pp'}(t)^\delta + \bar{\gamma}_{\mu\mu'}^{pp'}(t)$ as well by inserting (106) into (30)

$$\gamma_{\mu\mu'}^{pp'}(t) = [p' \gamma_\mu^\delta(t) + \bar{\gamma}_\mu(t)] \begin{cases} 1 & \text{for } \mu = \text{bosonic} \\ p' & \text{for } \mu = \text{fermionic} \end{cases} . \quad (109)$$

We have obtained the explicit dependence on the indices p and p' in this equation. Therefore we try to include these factors into the definition of the vertex

operators. Having included the γ_μ^δ -parts into the initial conditions, it turns out that closed RG equations can be found for the quantities

$$(G_\mu)_{ss',\dots} = \begin{cases} \sum_p (G_\mu^p)_{ss',\dots} & \text{for } N_s - N_{s'} = \text{even or } \mu = \text{bosonic} \\ -i \sum_p p (G_\mu^p)_{ss',\dots} & \text{otherwise} \end{cases}, \quad (110)$$

with N_s being the fermionic particle number of state s . In the same way we define the boundary vertices A_μ and B_μ . We have included a factor $-i$ for the second case in (110) in order to get the same symmetry relations as in (51)

$$(G_\mu)_{s_1 s'_1, s_2 s'_2}^* = (G_{\bar{\mu}})_{s'_1 s_1, s'_2 s_2}. \quad (111)$$

Using the fact that fermionic vertex operators $(G_\mu)_{ss',s_1 s'_1}$ change the parity of the fermionic particle number difference $N_{s_1} - N_{s'_1} \rightarrow N_s - N_{s'}$, we get after a lengthy but straightforward calculation the following RG-equations arising from the $\bar{\gamma}_\mu$ -parts

$$\begin{aligned} \frac{d}{dt_c} \tilde{\Sigma}(z) &= - \int_0^\infty dt \frac{d\bar{\gamma}_\mu}{dt_c}(t) A_{\bar{\mu}}(t) B_\mu \\ \frac{d}{dt_c} L_0 &= -i \int_0^\infty dt \frac{d\bar{\gamma}_\mu}{dt_c}(t) G_{\bar{\mu}}(t) G_\mu \\ \frac{d}{dt_c} G_\mu &= - \int_0^\infty dt \int_{-\infty}^0 dt' \frac{d\bar{\gamma}_{\mu_1}}{dt_c}(t-t') [\sigma_{\mu\mu_1} G_{\bar{\mu}_1}(t) G_\mu - G_\mu G_{\bar{\mu}_1}(t)] G_{\mu_1}(t') \\ \frac{d}{dt_c} A_\mu &= - \int_0^\infty dt \int_{-\infty}^0 dt' \frac{d\bar{\gamma}_{\mu_1}}{dt_c}(t-t') [\sigma_{\mu\mu_1} A_{\bar{\mu}_1}(t) G_\mu - A_\mu G_{\bar{\mu}_1}(t)] G_{\mu_1}(t') \\ \frac{d}{dt_c} B_\mu &= - \int_0^\infty dt \int_{-\infty}^0 dt' \frac{d\bar{\gamma}_{\mu_1}}{dt_c}(t-t') \sigma_{\mu\mu_1} G_{\bar{\mu}_1}(t) G_\mu B_{\mu_1}(t') \end{aligned}$$

(112)

where

$$\tilde{\gamma}_\mu(t) = \bar{\gamma}_\mu(t) \begin{cases} 1 & \text{for } \mu = \text{bosonic} \\ i & \text{for } \mu = \text{fermionic} \end{cases}, \quad (113)$$

and

$$\sigma_{\mu\mu'} = \begin{cases} 1 & \text{for } \mu \text{ or } \mu' = \text{bosonic} \\ -1 & \text{for } \mu \text{ and } \mu' = \text{fermionic} \end{cases}. \quad (114)$$

We see that the new RG equations are more compact but we note that they can not be applied to all models. Sometimes, like e.g. in spin boson models, it happens that the part $\gamma_\mu^\delta(t)$ can not be expressed by the derivative of a delta function and, consequently, can not be incorporated into the initial conditions. In this case, one should use the original and generally valid RG-equations (101).

5 Exact solution of the RG equations

In this section we demonstrate that the RG equations can be solved exactly for the special model (1)-(3) of a single non-degenerate dot state. It turns out that the result for the kernels agrees with that of section 3.2. We conclude that the RG-approach solves the present model exactly.

We choose the sharp cutoff-function $F(x) = \theta(x - 1)$ and get from the RG-equation (101) for a matrix element of the kernel

$$\tilde{\Sigma}(z)_{ss, \bar{s}\bar{s}} = \sum_{pp'\mu s'} \int_0^\infty dt_c \gamma_{\bar{\mu}\mu}^{pp'}(t_c) e^{izt_c} (A_{\bar{\mu}}^p)_{ss, s'\bar{s}'} e^{-i\alpha_{s'} t_c} (B_{\mu}^{p'})_{s'\bar{s}', \bar{s}\bar{s}} . \quad (115)$$

Here, due to particle number conservation, we have used the fact that the only nonvanishing matrix elements of L_0 are $\alpha_s = (L_0)_{s\bar{s}, s\bar{s}}$ and $(L_0)_{ss, s's'}$. To evaluate this equation we need the t_c dependence of α_s and the boundary vertex operators. To obtain this it is convenient to include the part γ_{μ}^{δ} into the initial conditions. The latter follow from inserting the part $\gamma_{\bar{\mu}\mu}^{pp'}(t_c)^{\delta}$ into the RG-equations (101), and integrating. We denote the initial value for L_0 by L_0^{δ} . The vertex operators do not obtain any initial renormalization from the δ -function parts since there is no phase space for the time integrals in (101). Taking the part $\gamma_{\bar{\mu}\mu}^{pp'}(t_c)^{\delta}$ from the first term of (109) together with (108), and inserting it in the RG-equation (101) for L_0 , we find

$$\left(\frac{d}{dt_c}\right)\alpha_s^{\delta} = i\frac{\Gamma}{2}\delta(t_c)pp'(G_{\bar{\mu}}^p G_{\mu}^{p'})_{s\bar{s}, s\bar{s}} = -i\Gamma\delta(t_c) . \quad (116)$$

This gives

$$\alpha_0^{\delta} = -\epsilon - i\frac{\Gamma}{2} \quad , \quad \alpha_1^{\delta} = \epsilon - i\frac{\Gamma}{2} , \quad (117)$$

where the part with the single particle energy ϵ stems from the initial value without any renormalization.

As we will show in the following we find no further renormalization from the $\tilde{\gamma}_{\mu}$ -part, i.e. using the simplified set of RG-equations (112), we get

$$\frac{d}{dt_c}\alpha_s = \frac{d}{dt_c}(A_{\mu})_{ss, s'\bar{s}'} = \frac{d}{dt_c}(B_{\mu})_{s'\bar{s}', \bar{s}\bar{s}} = \frac{d}{dt_c}G_{\mu} = 0 . \quad (118)$$

This means that the renormalization of the kernel due to the $\tilde{\gamma}_{\mu}$ -part can be calculated with unrenormalized vertex operators and using the result (117) for α_s . Since, trivially, the same applies to the γ_{μ}^{δ} -part, we can directly evaluate (115) in this way and get the result (74) of section 3.2.

What remains to be shown is Eq. (118). We first note the following properties of the matrix elements of the vertex operator, which follow from the definition (110)

$$\sum_s (G_{\mu})_{ss, s'\bar{s}'} = 0 \quad , \quad (G_{\mu})_{s\bar{s}, s's'} = (G_{\mu})_{s\bar{s}, \bar{s}'\bar{s}'} . \quad (119)$$

Furthermore, using (53), we get

$$\sum_s (e^{-iL_0 t})_{ss,\dots} = 1 . \quad (120)$$

We apply these properties to the following expression

$$\begin{aligned} [G_\mu(t)G_{\mu'}(t')]_{s\bar{s},s'\bar{s}'} &= \\ &= e^{i\alpha_s t} e^{-i\alpha_{s'} t'} \sum_{s_1 s_2} (G_\mu)_{s\bar{s},s_1 s_1} (e^{-iL_0(t-t')})_{s_1 s_1, s_2 s_2} (G_{\mu'})_{s_2 s_2, s' \bar{s}'} \\ &= e^{i\alpha_s t} e^{-i\alpha_{s'} t'} (G_\mu)_{s\bar{s},s_1 s_1} \sum_{s_2} (G_{\mu'})_{s_2 s_2, s' \bar{s}'} = 0 . \end{aligned} \quad (121)$$

Using this result after taking matrix elements of the RG-equations (112), we find immediately (118).

We conclude that after having set up the general RG-equations (101) and (112), the exact solution of the present model can be found analytically in a straightforward way. There is no need to consider diagrammatic details as in section 3.2. Furthermore, we see that the effect of the reservoirs is simply a broadening of the local state of the dot by $\Gamma/2$, see (117). Otherwise the evaluation of the kernel is the same as in lowest order perturbation theory in Γ .

6 Summary and outlook

In this article we have presented a new viewpoint to analyse nonperturbative aspects of nonequilibrium systems. We considered a small system coupled linearly to several baths. Nonperturbative means that the coupling between system and bath is so strong that quantum fluctuations induce broadening of the states in the system together with possible renormalization of energy levels and the coupling to the environment. In macroscopic systems, such effects are negligible since the interaction with the environment is a surface effect. In contrast, our goal is to describe mesoscopic systems like quantum dots, magnetic nanoparticles or chemical molecules coupled to particle or heat reservoirs. Usually such systems are treated within perturbation theory [14,15,16]. This means that the kernel $\Sigma(t)$ of the kinetic equation is calculated in lowest order perturbation theory in the coupling, the so-called golden rule or Pauli-Master equation approach. Our aim here was to find a systematic way to consider self-consistently an infinite series of higher-order contributions to the kernel. This is a nontrivial task, especially in nonequilibrium where a real-time formalism on a Keldysh contour has to be used. Renormalization effects known from equilibrium theories have to be incorporated consistently within a kinetic equation. Our point of view relies on renormalization group ideas. We try to integrate out all energy scales of the bath in infinitesimal steps. Each step is interpreted as a change of various quantities, like broadening and renormalization of energy levels, and generation of rates. For formal reasons we have set up this procedure in real-time space.

During this procedure we keep the kernel of the kinetic equation invariant and generate non-Hamiltonian dynamics to describe the physics of dissipation. The final RG-equations are presented in (101), and, alternatively, in (112). Solving them, provides the complete description of the time-evolution of the reduced density matrix of the system and arbitrary observables being linear in the field operators of the bath. This includes the consideration of an initially out of equilibrium state as well as the description of stationary nonequilibrium situations. We have solved the equations exactly for the special case of a quantum dot with one state coupled to two particle reservoirs. The solution turned out to be identical to the exact one.

The reader might argue that this is a trivial result since the model under consideration is very simple. However, as shown in a recent paper, the same RG equations provide not only the exact solution for a noninteracting quantum dot with one state, but gives a good solution also for the spin-degenerate case including a finite on-site Coulomb interaction U [1], the so-called Anderson impurity model in nonequilibrium. Here, not only energy broadening but also energy and coupling constant renormalizations are important. In the mixed-valence and empty-orbital regime, i.e. for level positions near or above the Fermi level of the reservoirs, it was shown that the linear conductance and the average occupation in equilibrium agrees perfectly with Friedel sum rules, Bethe ansatz, and numerical renormalization group methods within 2-3%. This means that the RG provides a good solution for the whole range from $U = 0$ to $U = \infty$. This is a surprising result since usually methods designed for strong interaction do not work well for weak interaction and vice versa. Therefore, the fact that the RG gives the exact result for the noninteracting case is not at all a trivial result. In fact, within the slave boson technique [17], which is a well-known and well-established method in the theory of strongly correlated Fermi systems, it is very complicated to find the exact solution for $U = 0$ [17].

Another example where the RG-method has been applied is the study of transport through the metallic single-electron transistor [18]. For this case, the RG-equations have been solved in sixth-order perturbation theory in the coupling. Surprisingly, it turned out that the solution agrees very well with exact perturbation theory in the same order. The reason why the RG-equations have not been solved in all orders is that the result was not finite for the band width cutoff $D \rightarrow \infty$. Only if certain parts of double-vertex corrections were included, the solution turned out to be cutoff-independent. A more detailed study of the D -dependence and the solution for higher orders is currently under way.

The RG-equations on the level of propagator and single-vertex renormalization are pure differential equations and, consequently, can be solved numerically very quickly. Typical response times range from seconds to a few minutes for one set of parameters, even on a usual PC machine. There are still some problems with the asymptotic solution of the RG equations for $t_c \rightarrow \infty$. First, it is not known rigorously whether a stationary solution exists at all. Secondly, the numerical solution is plagued by oscillating functions, typical for real-time problems. However, for the problems studied so far, and provided the coupling is not too

strong, there is a stationary numerical solution over a sufficiently long period in t_c . This applies at least to the physical quantities under consideration, like the probability distribution and the current.

Another reason for the efficiency of the present method is the possibility to calculate physical observables directly without the need of correlation functions like in linear response theory. Furthermore, if desired, correlation functions can also be studied with the RG-method. In this case, there are additional RG-equations to describe the renormalizations of the external vertices defining the correlation function. These equations together with explicit solutions will be published in forthcoming works.

The method is also applicable to the study of the ground state energy since the RG-flow on the single forward propagator provides the S-matrix. This idea has been applied to the single-electron box [10], coupled metallic islands [19], and the one-dimensional Polaron problem [20]. In the first two cases very good results have been obtained, even comparable to very time-consuming QMC-simulations. For the 1d-Polaron problem, the results were at least satisfactory for small coupling. Here, problems occurred since the correlation function of the bath does not decay for long times and undamped modes occur which make the numerical analysis of the asymptotic solution very difficult.

Finally, we remark that a challenge for future research is the consideration of higher-order vertex corrections. Our RG-scheme provides a systematic treatment for setting up RG-equations for all kinds of multiple vertices. However, even on the level of double-vertices, the number of terms increases considerably and the RG-equations become integral-differential equations. The reason is the retarded nature of double-vertices. Therefore it is necessary to find physical arguments to select the most important terms or to improve the numerical efficiency by neglecting the retardation in a convenient way. Whereas single-vertices describe basically charge fluctuations (in case of coupling to particle reservoirs), double-vertices describe physical processes via virtual intermediate states where the local system can change its state without changing its particle number. This is e.g. important for the study of spin fluctuations in local impurities or quantum dots, leading to the Kondo effect [8,12]. Although such processes are perturbatively included in the RG-equations set up in this article, it is important to study them fully self-consistently by considering corresponding RG-equations for double-vertex terms on a Keldysh contour.

7 Acknowledgements

Useful discussions are acknowledged with T. Costi, J.v. Delft, H. Grabert, G. Schön, K. Schönhammer, and P. Wölfle. I owe special thanks to J. König, T. Pohjola, and M. Keil for very fruitful collaborations on applying the RG-method to various systems. This article was supported by the Swiss National Science Foundation (H.S.) and by the "Deutsche Forschungsgemeinschaft" as part of "SFB 195".

Appendix

Here we prove Eqs.(62)-(64). The first one follows from

$$(\overline{G_\mu^+})_{ss,\bar{s}s} + (\overline{G_\mu^-})_{\bar{s}\bar{s},\bar{s}s} = 0, \quad (122)$$

which can easily be seen by using the definitions (27) and (28). The reservoir contraction is the same in both terms since G_μ^p is the vertex at later time, compare (31). The same proof can be used for I_μ^p by using the definition (37). Since there is no change of sign of I_μ^p if p is changed to \bar{p} , we have to add a factor p under the sum in (62).

To show the second property (63), we again use the definitions (27) and (28), and find

$$(\overline{G_\mu^p G_{\mu'}^{p'}})_{s\bar{s},..} + (\overline{G_\mu^{\bar{p}} G_{\mu'}^{\bar{p}'}})_{s\bar{s},..} = 0. \quad (123)$$

Both reservoir contraction are the same in both terms since both vertices are at later time. However, the reader can convince himself very easily that there is an additional relative sign between the two terms of (123) due to the interchange of reservoir Fermi operators.

The third property (64) follows from

$$\lim_{D \rightarrow \infty} \{(\overline{G_\mu^p G_{\mu'}^{p'}})_{s\bar{s},..} + (\overline{G_\mu^{\bar{p}} G_{\mu'}^{\bar{p}'}})_{s\bar{s},..}\} = 0. \quad (124)$$

Here, by comparing the two terms, the contraction associated with the second vertex changes from γ_r^η to $\gamma_r^{-\eta}$. Otherwise the two terms are the same. However, the sum $\gamma_r^\eta(t) + \gamma_r^{-\eta}(t)$ gives a $\delta(t)$ -function in the limit $D \rightarrow \infty$, see (26). This means that there is no phase space in time for the first vertex and the sum is zero.

References

1. H. Schoeller and J. König, cond-mat/9908404.
2. A.L. Fetter and J.D. Walecka, "Quantum Theory of Many Particle Systems", (McGraw-Hill, New York, 1971).
3. P.W. Anderson, J. Phys. C **3**, 2346 (1970); K.G. Wilson, Rev. Mod. Phys. **47**, 773 (1975).
4. H.R. Krishna-murthy, J.W. Wilkins, and K.G. Wilson, Phys. Rev. B **21**, 1003 (1980); Phys. Rev. **21**, 1043 (1980).
5. T.A. Costi, A.C. Hewson, and V. Zlatić, J. Phys. C **6**, 2519 (1994).
6. S.D. Glazek and K.G. Wilson, Phys. Rev. D **48**, 5863 (1993); F. Wegner, Ann. Physik (Leipzig), **3**, 77 (1994).
7. P. Joyez, V. Bouchiat, D. Esteve, C. Urbina, and M.H. Devoret, Phys. Rev. Lett. **79**, 1349 (1997).
8. D. Goldhaber-Gordon *et al.*, Nature (London), **391**, 156 (1998); Phys. Rev. Lett. **81**, 5225 (1998); S.M. Cronenwett *et al.*, Science **281**, 540 (1998); J. Schmid *et al.*, Physica B **256-258**, 182 (1998); F. Simmel *et al.*, Phys. Rev. Lett. **83**, 804 (1999).

9. H. Schoeller, in '*Mesoscopic Electron Transport*', eds. L.L. Sohn *et al.* (Kluwer 1997), p. 291; J. König, "Quantum Fluctuations in the Single-Electron Transistor", Shaker (Aachen, 1999).
10. J. König and H. Schoeller, Phys. Rev. Lett. **81**, 3511 (1998).
11. C. Caroli *et al.*, J. Phys. C **4**,916 (1971); J. Phys. C **5**, 21 (1972).
12. A.C. Hewson, *The Kondo Problem to Heavy Fermions*, (Cambridge University Press, 1993).
13. I. Affleck and A.W.W. Ludwig, Nucl. Phys. B **360**, 641 (1991).
14. K. Blum, *Density Matrix Theory and Applications*, 2nd edition (Plenum Press, 1996).
15. E. Fick and G. Sauermaun, *The Quantum Statistics of Dynamic Processes*, (Springer, 1990).
16. C.W. Gardiner, *Quantum noise*, Springer Series in Synergetics 56, (Springer-Verlag, Berlin, 1991).
17. S.E. Barnes, J. Phys. F: Metal Phys. **6**, 1375 (1976); **7**, 2637 (1977).
18. F. Kuczera, H. Schoeller, J. König, and G. Schön, submitted to Europhys. Lett..
19. T. Pohjola, J. König, H. Schoeller, and G. Schön, Phys. Rev. B **59**, 7579 (1999).
20. M. Keil and H. Schoeller, preprint 1999.